JOURNAL OF AIRCRAFT
Vol. 43, No. 6, November–December 2006

Engineering Notes

ENGINEERING NOTES are short manuscripts describing new developments or important results of a preliminary nature. These Notes should not exceed 2500 words (where a figure or table counts as 200 words). Following informal review by the Editors, they may be published within a few months of the date of receipt. Style requirements are the same as for regular contributions (see inside back cover).

Interaction of a Streamwise Vortex with a Blade Tip Vortex

T. Lee* and Y. Adukesem†
McGill University, Montreal, Quebec H3A 2K6, Canada

DOI: 10.2514/1.26324

Nomenclature

b	=	(semispan) wing span
c	=	chord
Re	=	chord Reynolds number
r_c	=	core radius
u	=	axial mean velocity
u_c	=	axial core velocity
u_d	=	core velocity deficit
u_o	=	freestream velocity
v_θ	=	tangential velocity
x, y, z	=	axial, normal and spanwise direction
Γ_c	=	core circulation
Γ_o	=	total circulation
Δ	=	separation distance
ζ	=	vorticity
κ	=	total turbulent kinetic energy

Introduction

THE tip vortices generated by aircraft wings, helicopter rotor blades, turbomachine blades, and wind turbine blades, to name a few, are known to be invariably associated with aerodynamic inefficiency and hazard. Extensive investigations have been conducted to better understand the tip vortex flow phenomena so as to improve the modeling and its control. Moreover, for rotorcraft, when these shed concentrated vortices interact with the trailing rotor blades, the unsteady pressure fluctuations induced on the blade surfaces generally lead to severe dynamic structural loading and impulsive blade-vortex interaction (BVI) noise generation. Two important BVI extremes occur when the vortex is either normal or parallel to the rotor blade. Normal BVI is also observed when the vortical wake shed by a finite span canard impinges on a wing [1]. However, despite the published measurements on steady-state normal BVIs [1–3], the direct interaction of a 3-D streamwise vortex with the blade tip and, subsequently, the blade tip vortex is scarce. The objective of the present study was to investigate the downstream development of a streamwise vortex interacted with a blade tip vortex at selected vortex–blade separation distances for $Re = 1.54 \times 10^5$. Special emphasis was placed on the quantification of the critical vortex flow parameters, such as vortex strength, size, geometry, and trajectory, as well as the vortex-induced turbulence flowfield, by using a miniature triple hot-wire probe.

Received 4 July 2006; revision received 18 August 2006; accepted for publication 22 August 2006.

*Associate Professor, Department of Mechanical Engineering.
†Research Assistant, Department of Mechanical Engineering.

Experimental Methods

The experiment was conducted in the low-turbulence suction wind tunnel at McGill University. The vortex generator was a sweptback wing with a taper ratio of 0.375 and a semiwing span b of 51 cm, and was mounted horizontally to the sidewall of the wind tunnel. The rectangular interaction blade, placed at $\alpha = 5$ deg, had a chord length c of 20 cm and $b = 50$ cm, and was mounted 2.75 root chords downstream of the trailing edge of the vortex generator. The origins of the coordinates are located at the leading edge of the interaction blade. The position of the interaction blade could be varied laterally to change the blade-vortex separation distance Δ, which is positive when the vortex passed on the suction side of the blade and negative when it passed on the pressure side. In the absence of the interaction blade, $\Delta = 0$ denotes that the center of the undisturbed generator vortex impinges the blade tip at the leading edge (i.e., at $x/c = 0$). Corresponding to 1 to 4.5 core radii of the undisturbed generator vortex at $x/c = 0$, $\Delta = \pm r_c$, $\pm 2r_c$, $\pm 3r_c$, and $4.5r_c$ were examined. Details of the experimental setup are given by Daccache and Lee [3].

Results and Discussion

To facilitate the investigation of the evolution of a streamwise vortex encountering a blade tip vortex, the three-dimensional flow structures of an undisturbed generator vortex for $x/c = -1.75$ to 3 were documented first and served as a comparison. Figures 1a–1c show the isocontours of $\zeta c/u_o$, u_d/u_o, and κ/u_o^2 $[= \frac{1}{2}(u'^2 + v'^2 + w'^2)/u_o^2]$ at $x/c = 0$. The majority of the vortex roll up, except the outer flow region, was nearly completed. The near completion of the roll up of the shear layers in the inner region of the vortex flow can also be demonstrated from the nearly axisymmetric distributions of v_θ, ζ, and u across the vortex center along the z axis (Fig. 1d). The variation of the critical vortex flow quantities with x/c is depicted in Fig. 2. The core radius r_u and u_c were found to increase with x/c (Figs. 2a and 2b), whereas the peak $v_{\theta,\text{peak}}$ and ζ_{peak} were decreased (Figs. 2c and 2d). On the other hand, a rather constant $\Gamma_c \approx 0.075cu_o$ and $\Gamma_o \approx 0.11cu_o$ were observed for $-0.75 < x/c \leq 3$ (Figs. 2e and 2f), which further suggests the near completion of the roll up of the inner region of the tip vortex with a Γ_c/Γ_o ratio of about 0.68 (compared with the theoretical value of 0.71 of Lamb's solution [4]). The circulation was calculated employing Stokes's theorem. Note that at $x/\text{c} = 0$ (i.e., at the time of the interaction of the generator vortex with the leading edge of the interaction blade), the generator vortex had already displayed a significant maturity with r_c, $v_{\theta,\text{peak}}$, u_c, Γ_c, and Γ_o equal to $0.078c$, $0.21u_o$, $0.935u_o$, $0.075u_oc$, and $0.16u_oc$, respectively.

The turbulence structure of the undisturbed generator vortex was also documented. The high κ level appeared in the core region implies that the core region could be turbulent (Fig. 1c). The vortex meandering in the low-turbulence wind tunnel was examined by using the correlation technique/criteria employed by Chow et al. [5]. It was determined from the correlation measurements that meandering of the vortex was very small and did not contribute noticeably to the present measurements. Note that Ramaprian and Zheng [6] further suggested that the effects of vortex wandering only gains significance in the far field. The maximum $\kappa_{\max}/u_o^2$ in the

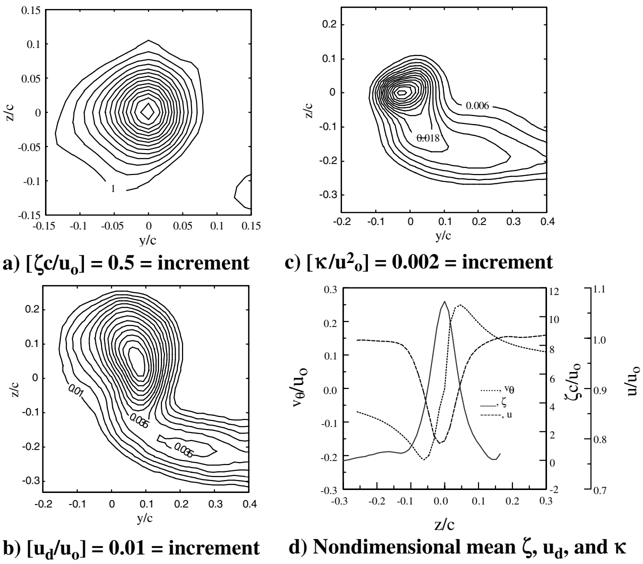

a) $[\zeta c/u_o] = 0.5$ = increment
c) $[\kappa/u_o^2] = 0.002$ = increment
b) $[u_d/u_o] = 0.01$ = increment
d) Nondimensional mean ζ, u_d, and κ

Fig. 1 Contours of an undisturbed generator vortex at $x/c = 0$ (for Figs. 1a–1c). Numerical values denote contour levels.Vortex flow distribution at $x/c = -1.75$ (for Fig. 1d).

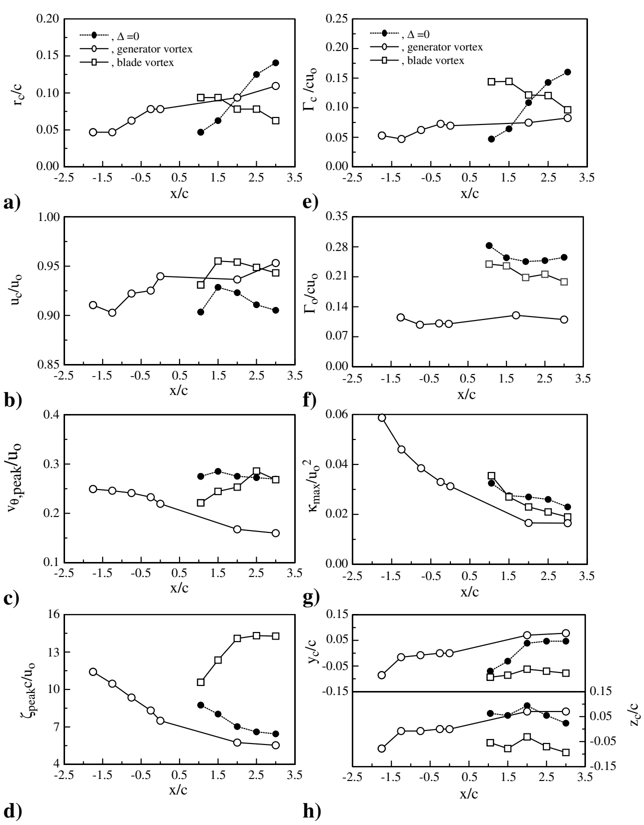

Fig. 2 Variation of critical interaction vortex flow quantities with x/c.

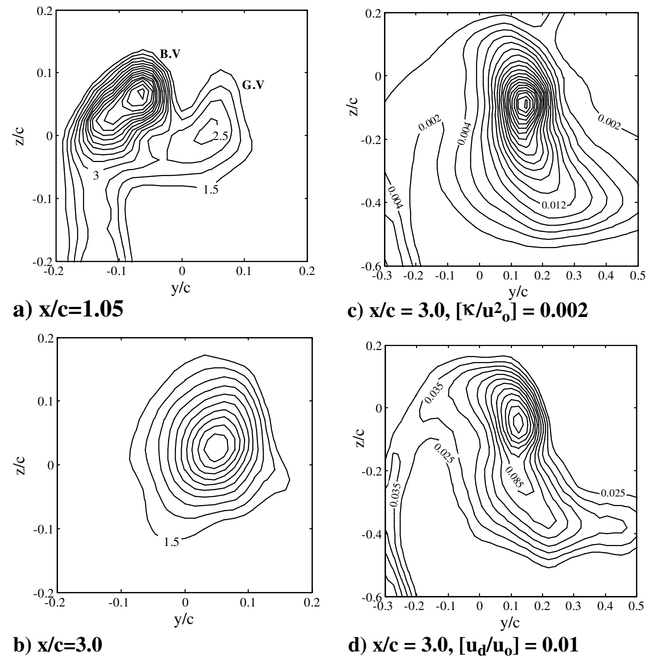

a) x/c=1.05
c) x/c = 3.0, $[\kappa/u_o^2] = 0.002$
b) x/c=3.0
d) x/c = 3.0, $[u_d/u_o] = 0.01$

Fig. 3 Typical contours of nondimensional vorticity, axial velocity deficit, and total turbulent kinetic energy for $\Delta = 0$; $\zeta c/u_o$ increment is 0.5.

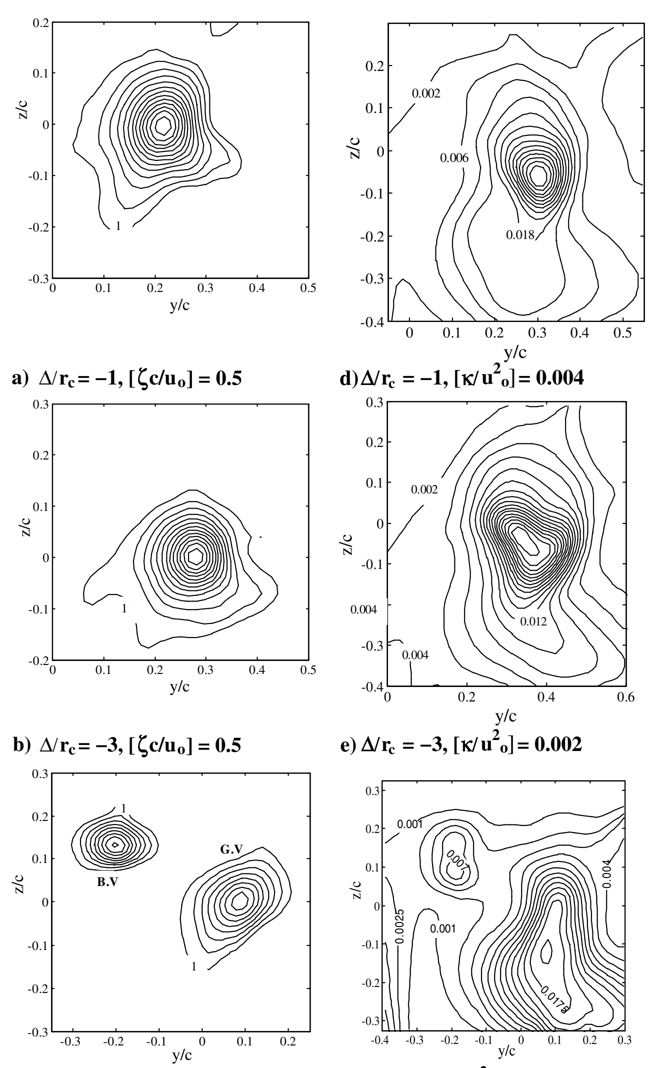

a) $\Delta/r_c = -1$, $[\zeta c/u_o] = 0.5$
d) $\Delta/r_c = -1$, $[\kappa/u_o^2] = 0.004$
b) $\Delta/r_c = -3$, $[\zeta c/u_o] = 0.5$
e) $\Delta/r_c = -3$, $[\kappa/u_o^2] = 0.002$
c) $\Delta/r_c = 3$, $[\zeta c/u_o] = 0.5$
f) $\Delta/r_c = 3$, $[\kappa/u_o^2] = 0.0015$

Fig. 4 Contours of nondimensional vorticity, axial velocity deficit, and total turbulent kinetic energy at $x/c = 3.0$ for $\Delta \neq 0$.

vortex core was also seen to decay quite strongly as the tip vortex progressed downstream (Fig. 2g).

The direct interaction of the generator vortex with the blade tip (i.e., $\Delta = 0$) and, subsequently, the corotating blade tip vortex for $x/c = 1.05$ to 3 was investigated. For $x/c < 1.05$, the disturbing vortex and the blade tip vortex, which had just rolled up, can be recognized very clearly. These two distinct vortices orbited each other between $x/c = 1.05$ (Fig. 3a) and 1.5. Further downstream, the passing generator vortex was entrained into the evolving blade vortex and merged into a single and enlarged vortex of elevated turbulence levels and tangential velocities (Fig. 3b). The downstream development of the circumferentially averaged critical vortex flow

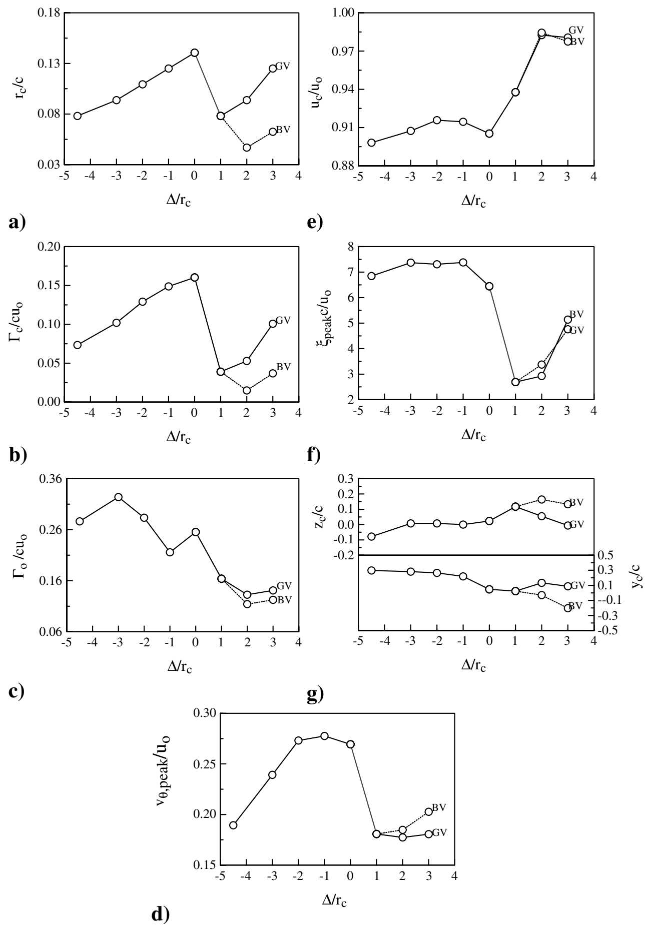

Fig. 5 Effect of Δ on critical vortex flow quantities.

quantities of the interaction vortex for $\Delta = 0$ is summarized in Fig. 2. Figures 2c and 2f show that $v_{\theta,\mathrm{peak}}$ and Γ_o of the interaction vortex were of values above the undisturbed generator vortex (and the undisturbed blade vortex as well), and were insensitive to the variation in x/c with $v_{\theta,\mathrm{peak}} \approx 0.27u_o$ and $\Gamma_o/cu_o \approx 0.245$ for $1.05 < x/c \leq 3$ (Figs. 2c and 2f). The peak vorticity, however, was found to decrease slightly with x/c (for $x/c > 1$) and had values above the generator vortex (Fig. 2e). The axial core velocity u_c varied slightly with x/c and was of the lowest value compared with the undisturbed vortices (Fig. 2b). Note that although $v_{\theta,\mathrm{peak}}$ of the interaction vortex remained basically constant, Γ_c and r_c were found to increase drastically and approximately linearly with x/c (Figs. 2a and 2e). Additionally, the vortex was found to be shifted slightly further inboard and toward the suction side of the interaction blade (Fig. 2h), compared with an undisturbed vortex, and interacted constructively with a blade-generated vortex of the same sign to create a field of a stronger interaction vortex (i.e., a constructive mode). Figure 3c also indicates that, similar to an undisturbed passing vortex, the levels of κ/u_o^2 and $\kappa_{\max}/u_o^2$ (Fig. 2g) were found to decrease as the vortex progressed downstream, but were persistently higher than the undisturbed vortices. Also shown in Fig. 3d are the u_d/u_o contours at $x/c = 3$.

The effects of blade-vortex separation distance on the flow structures of the interaction vortex for $\Delta = \pm r_c, \pm 2r_c, \pm 3r_c$, and $-4.5r_c$ or $\Delta = \pm 0.078c, \pm 0.156c, \pm 0.234c$, and $0.351c$ were also examined at $x/c = 3$. Figure 4 displays the representative isocontours of $\zeta c/u_o$ and κ/u_o^2 for $\Delta/r_c = -1$ and ± 3. The $\zeta c/u_o$ contours clearly indicate that for $\Delta < 0$, the vortex interaction was significant and the passing generator vortex (GV) and the blade tip vortex (BV) merged into a single interaction vortex (i.e., a constructive mode; see Figs. 4a and 4b). For $\Delta/r_c > 1$, two corotating vortices (i.e., GV and BV), however, were formed (i.e., a pairing mode; see Fig. 4c) with the center-to-center separation distance increased with increasing Δ. For $\Delta/r_c < 1$, a combined vortex structure, with a primary vortex outboard of the blade tip and a much weaker secondary vortex, located closer to or inboard of the blade tip, of the same sign, appeared. The turbulence levels were consistently larger for $\Delta < 0$ compared with the $\Delta > 0$ data (Figs. 4d–4f). The significant influence of Δ on the critical vortex flow quantities at $x/c = 3$ is summarized in Fig. 5. For $\Delta \leq 0$, the size and strength of the interaction vortex (i.e., r_c and Γ_c) increased linearly with decreasing $|-\Delta|$ (Figs. 5a and 5b), whereas Γ_o was found to be generally decreased with increasing $|-\Delta|$ (Fig. 5c). The peak tangential velocity was increased somewhat nonlinearly with decreasing $|-\Delta|$ (Fig. 5d), whereas the magnitudes of u_c and ζ_{peak} remained virtually unchanged (Figs. 5e and 5f). In contrast to the $\Delta < 0$ data, there was a drastic reduction in r_c, Γ_c, $v_{\theta,\mathrm{peak}}$, and ζ_{peak} for $0 < \Delta/r_c \leq 1$. No significant discrepancy in Γ_o, u_c, $v_{\theta,\mathrm{peak}}$, and ζ_{peak} between these two corotating vortices, however, was found for $\Delta/r_c > 1$; the core radius and Γ_c of the generator vortex were found to increase considerably with increased positive Δ and were of higher values than the blade vortex. The vortex center remained insensitive to Δ for $\Delta/r_c < -1$, while it began to shift further inboard and onto the pressure side of the interaction blade with increasing positive Δ (Fig. 5g).

Conclusions

The downstream development of a streamwise vortex interacted with a blade tip vortex was investigated. For $\Delta = 0$, the peak tangential velocity of the interaction vortex remained basically unchanged, whereas Γ_c and r_c were increased approximately linearly with x/c. For $\Delta < 0$, the generator vortex interacted constructively with the blade tip vortex of the same sign to create a single and stronger interaction vortex (i.e., a constructive mode). The values of r_c, Γ_c, and $v_{\theta,\mathrm{peak}}$ of the interaction vortex increased with reducing $|-\Delta|$ and exhibited a local maximum at $\Delta = 0$. For $\Delta > r_c$, the passing generator vortex paired with the blade vortex of the same sign to create a field of a vortex pair (i.e., a pairing mode) with the generator vortex of larger r_c and Γ_c, but lower $v_{\theta,\mathrm{peak}}$ than the blade vortex.

Acknowledgments

The work was supported by the Natural Science and Engineering Research Council (NSERC) of Canada.

References

[1] Khan, F. A., and Mueller, T. J., "Tip Vortex/Airfoil Interaction for a Low Reynolds Number Canard/Wing Configuration," *Journal of Aircraft*, Vol. 28, No. 3, 1991, pp. 181–186.
[2] Wittmer, K. S., Devenport, W. J., Rife, M. C., and Glegg, S. A., "Perpendicular Blade Vortex Interaction," *AIAA Journal*, Vol. 33, No. 9, 1995, pp. 1667–1674.
[3] Daccache, E., and Lee, T., "Effect of a Winglet on Normal Blade-Vortex Interaction," *Journal of Aircraft* (to be published).
[4] Lamb, H., *Hydrodynamics*, 6th ed., Dover, New York, 1945, p. 592.
[5] Chow, J. S., Zilliac, G. G., and Bradshaw, P., "Mean and Turbulence Measurements in the Near Field of a Wingtip Vortex," *AIAA Journal*, Vol. 35, No. 10, 1997, pp. 1561–1567.
[6] Ramaprian, B. R., and Zheng, Y., "Measurements in Rollup Region of the Tip Vortex from a Rectangular Wing," *AIAA Journal*, Vol. 35, No. 12, 1997, pp. 1837–1843.